



NRC Publications Archive Archives des publications du CNRC

The process of failure of columnar-grained ice Gold, L. W.

This publication could be one of several versions: author's original, accepted manuscript or the publisher's version. /
La version de cette publication peut être l'une des suivantes : la version prépublication de l'auteur, la version
acceptée du manuscrit ou la version de l'éditeur.

Publisher's version / Version de l'éditeur:

Philosophical Magazine, 26, 2, pp. 311-328, 1972-08

NRC Publications Record / Notice d'Archives des publications de CNRC:

<https://nrc-publications.canada.ca/eng/view/object/?id=988456e9-e073-4009-bb50-572a6ca99a16>
<https://publications-cnrc.canada.ca/fra/voir/objet/?id=988456e9-e073-4009-bb50-572a6ca99a16>

Access and use of this website and the material on it are subject to the Terms and Conditions set forth at

<https://nrc-publications.canada.ca/eng/copyright>

READ THESE TERMS AND CONDITIONS CAREFULLY BEFORE USING THIS WEBSITE.

L'accès à ce site Web et l'utilisation de son contenu sont assujettis aux conditions présentées dans le site

<https://publications-cnrc.canada.ca/fra/droits>

LISEZ CES CONDITIONS ATTENTIVEMENT AVANT D'UTILISER CE SITE WEB.

Questions? Contact the NRC Publications Archive team at
PublicationsArchive-ArchivesPublications@nrc-cnrc.gc.ca. If you wish to email the authors directly, please see the
first page of the publication for their contact information.

Vous avez des questions? Nous pouvons vous aider. Pour communiquer directement avec un auteur, consultez la
première page de la revue dans laquelle son article a été publié afin de trouver ses coordonnées. Si vous n'arrivez
pas à les repérer, communiquez avec nous à PublicationsArchive-ArchivesPublications@nrc-cnrc.gc.ca.



Ser
THL
N21r2
no. 523
c. 2

ANALYZED

2510

BLDG

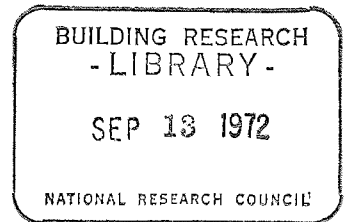
NATIONAL RESEARCH COUNCIL OF CANADA
CONSEIL NATIONAL DE RECHERCHES DU CANADA

THE PROCESS OF FAILURE OF
COLUMNAR-GRAINED ICE

by

L. W. Gold

Reprinted from
PHILOSOPHICAL MAGAZINE
Vol. 26, No. 2, August 1972
p. 311



Research Paper No. 523
of the
Division of Building Research

OTTAWA
August 1972

Price 25 cents

NRCC 12648

LE MECANISME DE DEFAILLANCE DANS LA GLACE GRANULAIRE EN COLONNES

par

L. W. Gold

Résumé

L'auteur rapporte des observations sur le fissurement qui se produit durant le cheminement, dû à la compression, de la glace granulaire en colonnes lorsque l'axe de la symétrie hexagonale de chaque grain tend à reposer dans le plan perpendiculaire à sa longueur. La nature de la glace et la direction de la contrainte par rapport aux grains en colonnes entraînent un comportement de déformation et une fissuration à deux dimensions. Les fissures produites sont des fissures de clivage, longues et étroites, et ne comprennent normalement qu'un ou deux grains. L'étude présente des renseignements sur la dépendance de la densité de fissure et du taux de fissuration (c.-à-d. le nombre de fissures par cm^2 par unité de contrainte) à l'égard de la déformation, de la contrainte et de la température. On a constaté que la fissuration se produit lorsque la contrainte de compression dépasse environ 6 kg/cm^2 . Pour une contrainte se situant entre 6 et 10 kg/cm^2 environ la fissuration se produit en grande partie durant le cheminement primaire. Si la contrainte est supérieure à environ 12 kg/cm^2 , la détérioration de la structure due à la fissuration transforme directement le cheminement primaire en cheminement tertiaire. Enfin, on examine les résultats obtenus en ce qui concerne le comportement de déformation de la glace.

CISTI / ICIST



3 1809 00211 3972

The Process of Failure of Columnar-grained Ice

By L. W. GOLD

Division of Building Research, National Research Council of Canada,
Ottawa, Canada

[Received 15 July 1971 and in revised form 1 January 1972]

ABSTRACT

Observations are reported on the cracking activity during compressive creep of columnar-grained ice with the axis of hexagonal symmetry of each grain tending to lie in the plane perpendicular to its long direction. Because of the nature of the ice and the direction of the stress relative to the columnar grains, the deformation behaviour and cracking activity were two-dimensional in nature. The cracks that formed were of the cleavage type, long and narrow, and usually involving only one or two grains. Information is presented on the strain, stress and temperature dependence of the crack density, and cracking rate (i.e. number of cracks per cm^2 per unit strain). It was found that crack formation takes place when the compressive stress exceeds about 6 kg/cm^2 . For stress between 6 and about 10 kg/cm^2 , most of the cracking activity occurs during primary creep. If the stress is greater than about 12 kg/cm^2 , deterioration of the structure due to the cracking activity causes the primary stage of creep to be transformed directly to the tertiary stage. The strain dependence of the crack density indicates the existence of two independent families of cracks, each obeying Weibull statistics. The implications of this for the ductile to brittle transition in ice are discussed.

§ 1. INTRODUCTION

It is well known that a material can break down gradually during deformation due to the formation of internal cracks. This behaviour has been discussed by Kenny and Campbell (1967) for metals; Jones (1962) for concrete; Brace, Paulding and Scholtz (1966) for rocks; and Gold (1960) for ice. Experiments were undertaken to determine the stress, strain, time and temperature dependence of this cracking activity for ice during compressive creep. The results of this study are reported here.

§ 2. STRUCTURE OF THE ICE

The ice used was prepared from the Ottawa city water supply. No steps were taken to purify the water except to deaerate it before freezing. Its electrical conductivity prior to freezing was about $137 \mu\text{mho}$ and the conductivity of the water obtained by melting the ice about $7 \mu\text{mho}$.

The water was cooled in a plastic-lined container about 60 cm in diameter and 60 cm deep. A pressure relief system was used to ensure that there was no buildup of pressure from expansion caused by freezing.

Freezing was initiated between 12 and 24 hours after deaerating by spreading finely crushed ice on the surface of the water, and was unidirectional, except close to the sides of the tank. Deaerating allowed the ice to grow to a thickness of more than 10 cm before visible air bubbles formed in it. The ice had a columnar-grained structure with the long direction of the columns in the direction of freezing.

Ice has hexagonal crystallographic symmetry. Hillig (1958) has shown that it has a marked tendency to grow more readily in directions perpendicular to the axis of symmetry than parallel to it. Because of the method used to initiate freezing, each grain initially had a random crystallographic orientation. Those grains that were favourably oriented with respect to the growth direction, however, soon squeezed out those that were unfavourably oriented. This behaviour is described and discussed by Ramseier (1968).

Within 3 cm of the surface there was a marked preference for the survival of only those grains with their axis of symmetry perpendicular to the direction of growth. This bias in crystallographic orientation became more pronounced as freezing progressed. The axis of hexagonal symmetry [0001] tended to have a random orientation in the plane perpendicular to the long direction of the columnar grains.

The cross-sectional area perpendicular to the long direction of the grains tended to increase in the direction of freezing. It ranged from about 0.14 cm²/grain to 0.28 cm²/grain. The average size as determined by the linear intercept method was 0.30 cm.

§ 3. PREPARATION OF SPECIMENS

Rectangular specimens, 5 × 10 × 25 cm³, were used for the tests. These specimens were cut so that the long direction of the grains was perpendicular to the 10 × 25 cm² face. A milling machine was used to bring them to their final dimensions. The specimens were stored in kerosene after milling to prevent sublimation. They were maintained at the test temperature for at least 48 hours before being tested.

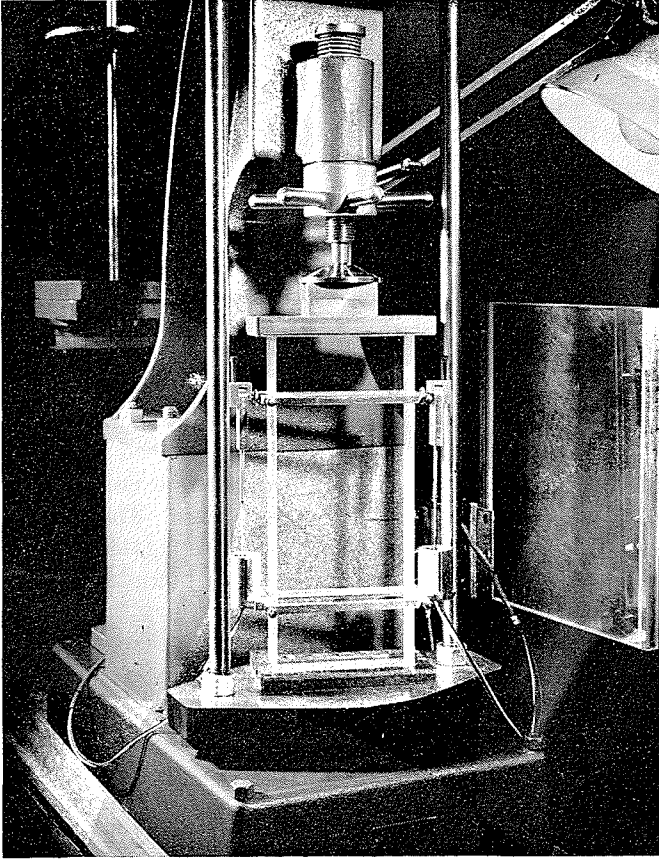
§ 4. LOADING PROCEDURE

A simple lever-type loading frame was used to apply constant compressive loads to the 5 × 10 cm² face of the specimens (i.e. perpendicular to the long dimension of the grains). Six tests were carried out for each stress condition at temperatures of -4.8°C, -9.5°C and -14.8°C and four tests were carried out for each load at the temperature of -31°C. The loads covered the stress range of 6 to 20 kg/cm² (5.9×10^5 to 19.5×10^5 N/m²). They were applied within 2 sec by lowering a jack which supported the appropriate weight.

Creep was measured with linear differential transformers attached to collars frozen to the ice. A special jig was used to locate the collars on the specimens when freezing them in place. The gauge length was 15.25 cm.

Two transformers were used, one mounted on each side of the specimen. The output from the transformers was recorded on a strip chart recorder or data logging system. The loading frame, with a specimen and extensometer in place, is shown in fig. 1.

Fig. 1



Loading frame with specimen and extensometer.

The loading frame was calibrated with a Baldwin SR-4 load cell, and the differential transformers with a displacement gauge accurate to 10^{-4} cm. Strains were measured to an accuracy better than 10^{-5} . The experiments were conducted in a cold room with temperature variation less than ± 0.25 c degree.

§ 5. CHARACTERISTICS OF CRACK FORMATION

It is known from experiment that it is much more difficult to induce slip on non-basal planes of ice than on basal planes. Evidence from experiment also indicates that there is no strongly preferred slip direction in the

basal plane (Kamb 1961). Because of the columnar-grained structure of the ice used in the present study, the preferred crystallographic orientation and direction of loading, the resolved shear stress on the basal plane in the long direction of each grain tended to be zero. Each grain had in effect only one independent slip system for deformation when the load was first applied. This system operated in the basal plane in a direction perpendicular to the long axis of the grains. Some of the consequences of this crystallographic and stress arrangement have been discussed by Gold (1966, 1970).

One of these was that the deformation was essentially two-dimensional for at least the first two per cent strain (i.e. the deformation occurred in the plane perpendicular to the long axis of the grains). The combination of a columnar-grained structure, one independent slip system, and two-dimensional deformation in a transparent solid provided a unique opportunity for a study of crack formation and the development of failure.

The cracks formed under the conditions of the experiments were long and narrow, with the ratio of length to width for the plane of the crack being greater than 3 : 1. Their long direction was in the long direction of the grains, and their plane tended to be parallel to the direction of the compressive stress. The cracks usually involved only one or two grains. In an earlier study by Gold (1966) it was observed that about three-quarters of the cracks formed during compressive creep at -9.5°C , for stress less than 20 kg/cm^2 , were transcrystalline. There was a marked tendency for the transcrystalline cracks to propagate either parallel or perpendicular to the basal planes. For grain boundary cracks, usually one or both of the grains making up the boundary had the basal plane parallel or perpendicular to it. These observations showed that the cracks tended to be cleavage cracks, and to form in or adjacent to grains that could not conform readily to the imposed deformation.

The formation of a crack had the characteristics of a local brittle event. There was no visual evidence of extension of cracks after they had formed. The cracks were made easily visible by directing a beam of light through the specimen so that it was reflected from their surface.

Cracks were observed visually. A count was made of the number of cracks formed in consecutive time intervals. The interval depended on the load and stage of the test. For large stresses the interval was usually one minute; for intermediate and smaller stresses longer intervals were used, and the location of counted cracks noted on the surface with a marking pencil. No distinction was made between cracks of different size. Only those cracks that formed within the gauge length were counted. Each experiment yielded for given load and temperature the time dependence of the strain and cracking activity.

Because of the two-dimensional nature of the deformation and crack formation, cracking activity was expressed as the number of cracks formed per unit area of specimen at a given time or strain. When this crack density exceeded about 3 per cm^2 , it became increasingly difficult to record

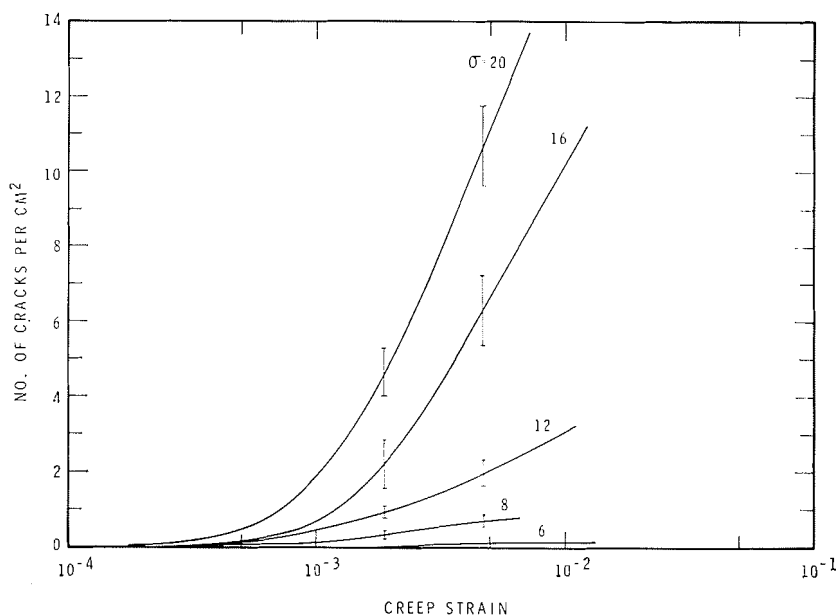
all cracking events. This was particularly the case for the larger loads. A true record of the cracking activity for a specimen containing many cracks was beyond the capability of visual methods. It is considered that the observations for densities less than 3 per cm^2 are a good record of the cracking activity. Observations at larger densities probably underestimate the cracking activity, but do give a good qualitative evaluation of it.

§ 6. OBSERVATIONS

A preliminary analysis of the observations showed that it was more meaningful to relate the cracking activity to strain than to time. Crack densities for each test, N , were plotted against creep strain. The average strain dependence of the crack density was calculated from these plots for given stress and temperature, and these are shown in figs. 2 (a), (b), (c) and (d). Standard deviations presented with the curves show the extent to which the behaviour was reproducible.

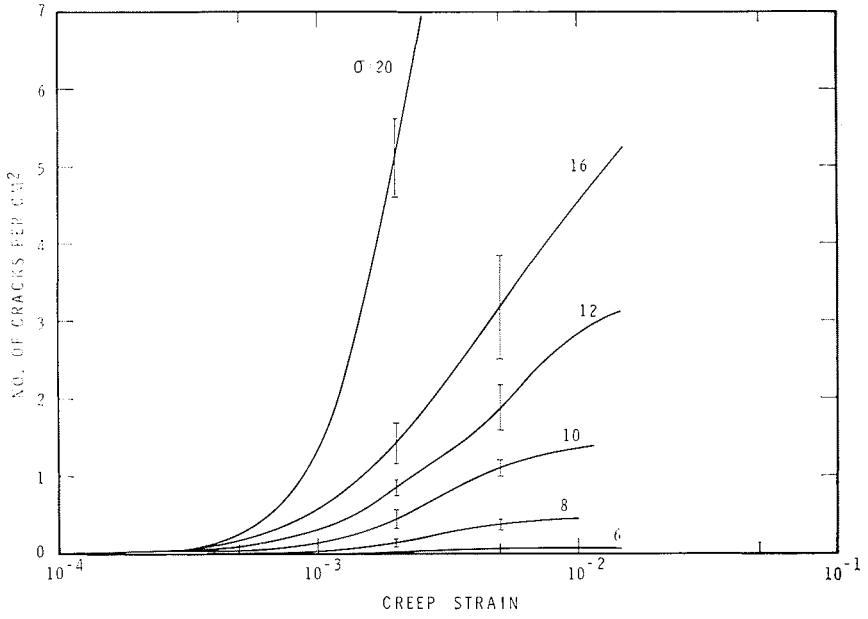
The average cracking rates (number of cracks per square centimetre per unit strain) were calculated from the average strain dependence of the crack density by determining the change in density for change in strain of 5×10^{-4} , dividing the difference by the change in strain, and plotting

Fig. 2

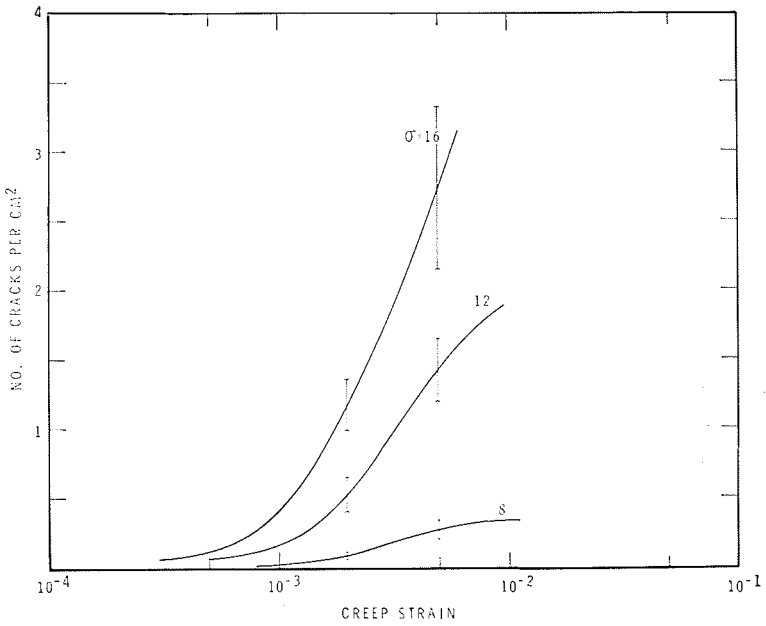


(a)

Fig. 2 (continued)

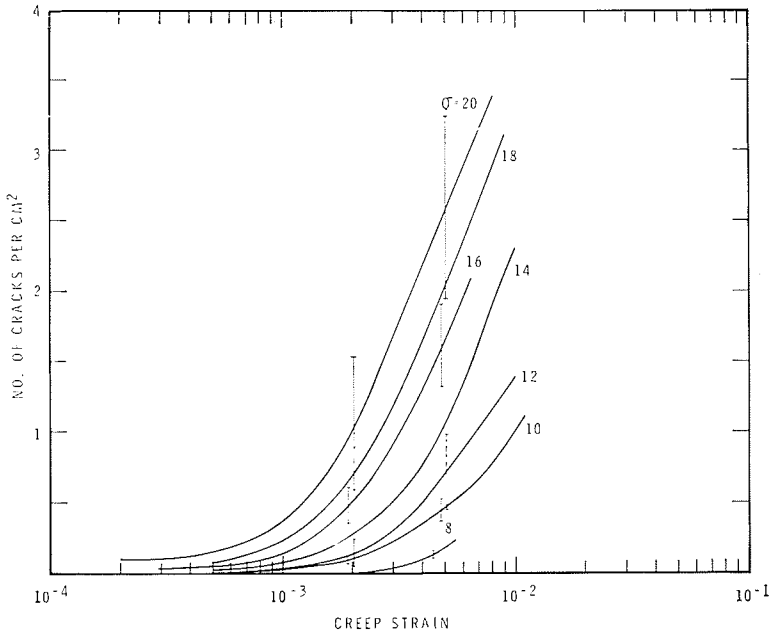


(b)



(c)

Fig. 2 (continued)



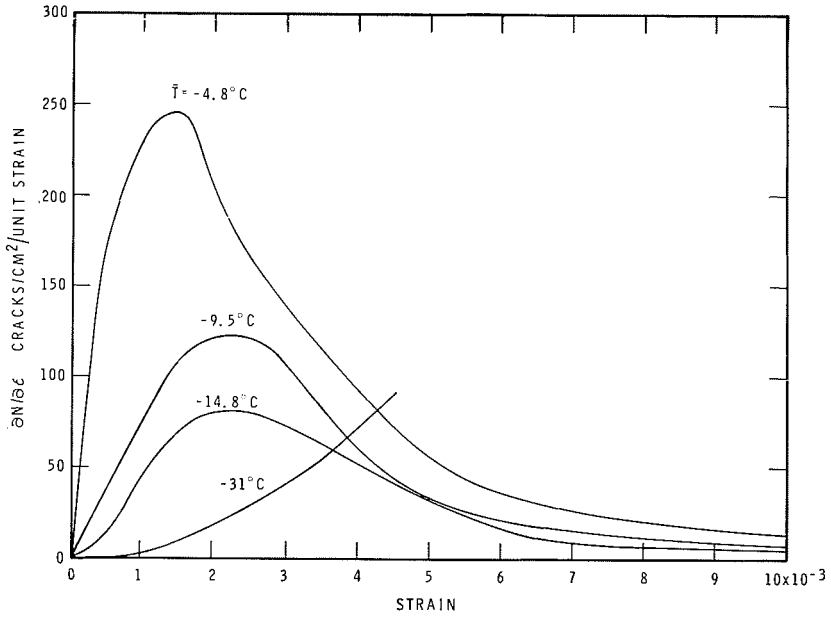
(d)

- (a) Strain dependence of crack density for compressive stress σ kg/cm²; $\bar{T} = -4.8^\circ\text{C}$. The height of the vertical bars is twice the standard deviation in the observations. (b) Strain dependence of crack density for compressive stress σ kg/cm²; $\bar{T} = -9.5^\circ\text{C}$. The height of the vertical bars is twice the standard deviation in the observations. (c) Strain dependence of crack density for compressive stress σ kg/cm²; $\bar{T} = -14.8^\circ\text{C}$. The height of the vertical bars is twice the standard deviation in the observations. (d) Strain dependence of crack density for compressive stress σ kg/cm²; $\bar{T} = -31^\circ\text{C}$. The height of the vertical bars is twice the standard deviation in the observations.

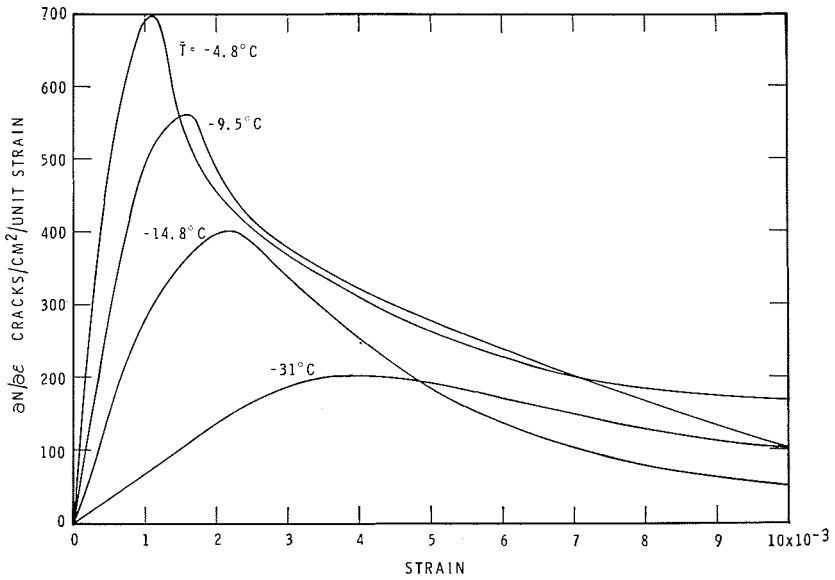
the result at the midpoint of the range. Smooth curves were drawn through the plotted points. These curves are presented in figs. 3(a), (b) and (c) for stresses of 8, 12 and 16 kg/cm².

In fig. 4 are presented the general characteristics of the creep behaviour. It can be seen that over the stress range of 10 to 12 kg/cm² there is a marked transition in this behaviour. For stresses less than 10 kg/cm² there occurred primary, secondary and, if the load was applied long enough, tertiary stages of creep. The transition from the primary to the secondary stage occurred when the strain was about 10^{-2} . When the stress was greater than 12 kg/cm², the primary stage was followed directly by the tertiary stage. There was usually a period of increasing creep rate during primary creep immediately after the application of the load. This has

Fig. 3

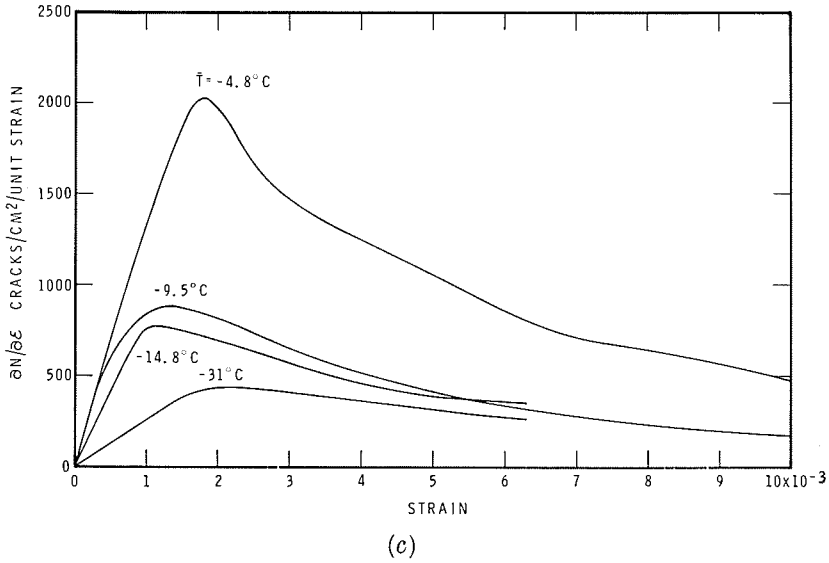


(a)



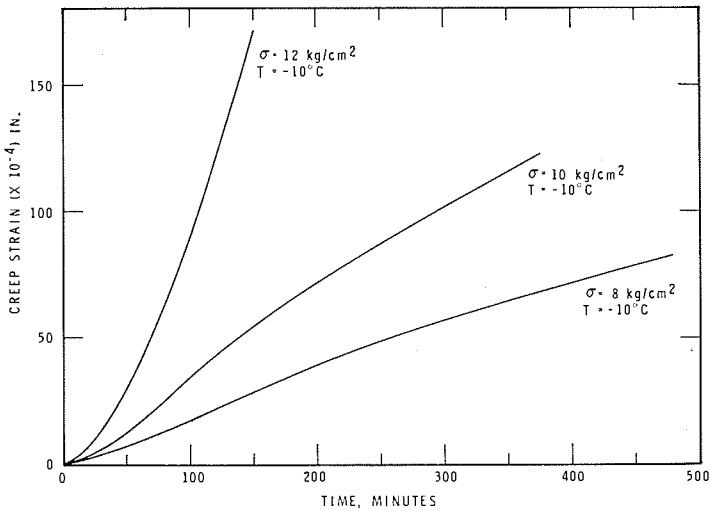
(b)

Fig. 3 (continued)



- (a) Strain dependence of the average rate of crack formation $\partial N/\partial \epsilon$; $\sigma = 8 \text{ kg/cm}^2$. (b) Strain dependence of the average rate of crack formation $\partial N/\partial \epsilon$; $\sigma = 12 \text{ kg/cm}^2$. (c) Strain dependence of the average rate of crack formation, $\partial N/\partial \epsilon$; $\sigma = 16 \text{ kg/cm}^2$.

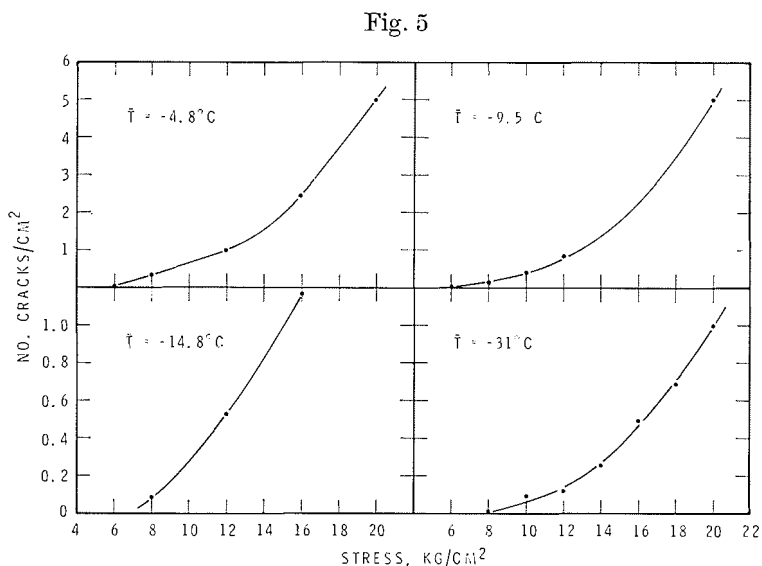
Fig. 4



Creep behaviour of columnar-grained ice.

been discussed by Gold (1965) and is considered to be associated with the development of new modes of deformation in previously undeformed columnar-grained ice.

The stress dependence of the average crack density for strain of 20×10^{-4} is shown in fig. 5. Figure 6 gives the observed temperature dependence of the density for given stress and strain.



Stress dependence of crack density at strain of 20×10^{-4} .

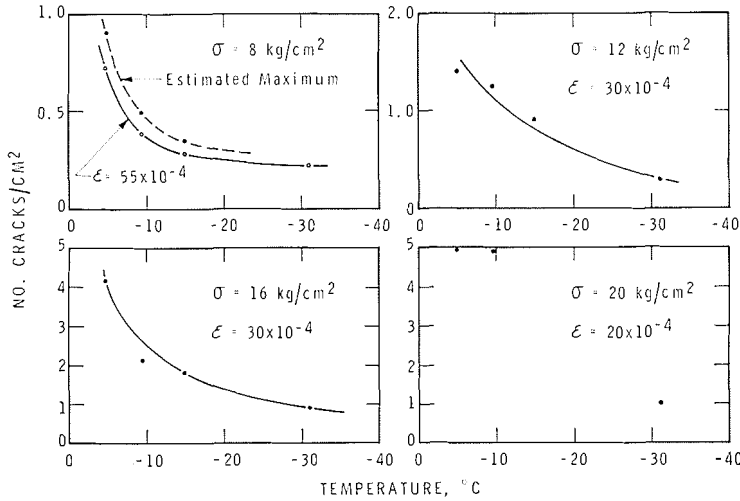
When the stress exceeded a fairly critical value, depending on the temperature, cracks formed in the specimen as it was loaded. These cracks were usually small, and associated with grain boundaries. There was a quiescent period after their formation, the length of which decreased with increase in stress. The stress dependence of this initial crack density is shown in fig. 7.

The initial cracking activity was subtracted from the total crack count when calculating the crack densities shown in fig. 2 because they formed during the development of the elastic strain on loading rather than while the specimen was creeping. Subtraction of these cracks did not affect the calculation of the average cracking rates, but did cause a downward displacement of the curves in fig. 2 that was less than 5% of the maximum observed densities for stress less than or equal to 16 kg/cm².

The observations brought out the following points:

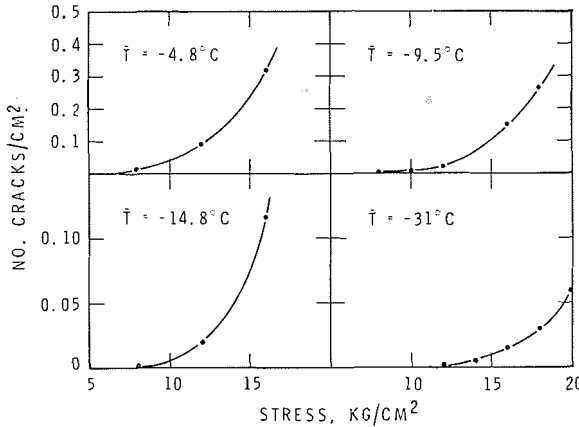
1. Significant cracking activity did not occur for the columnar-grained ice used in this study until the compressive stress exceeded about 6 kg/cm² (see fig. 5). Several tests were run at stresses less than 6 kg/cm² to determine whether cracks would form. Cracks did form in some cases for

Fig. 6



Temperature dependence of crack density for given stress and strain.

Fig. 7



Stress dependence of initial crack density.

stresses of 4 and 5 kg/cm², but these were few and small. They tended to heal with continued deformation, or collapse into several spherical voids, indicating that they were unstable.

2. The initiation and development of the cracking activity occurred over the same range of strain for all stress and temperature conditions (see figs. 2 (a), (b), (c) and (d)).

3. For stress $\leq 10 \text{ kg/cm}^2$, most of the cracking activity was confined to the primary stage of creep (i.e. strain $< 10^{-2}$). It was observed that

there was relatively little if any cracking activity during the secondary creep stage (see fig. 3 (a)).

4. For stresses $\geq 12 \text{ kg/cm}^2$, cracking activity was significant for the full period of the test (see figs. 3 (b), (c)).

5. There was a maximum in the cracking rate for all stresses which occurred in the strain range of 10×10^{-4} to 35×10^{-4} (i.e. in the primary stage of creep; see figs. 3 (a), (b) and (c)).

The result for $T = -31^\circ\text{C}$ and stress of 8 kg/cm^2 is inconsistent with those for the other test conditions. This may be due to the small number of cracks that formed for this condition, and the corresponding decrease in statistical significance. Although these particular tests were run for $3\frac{1}{2}$ days, it can be seen in fig. 3 (a) that the cracking rate had not reached its maximum value.

6. The cracking rate and total number of cracks formed at a given strain for given stress decreased with decrease in temperature (see figs. 3 (a), (b), (c) and fig. 6). The results for stress of 8 kg/cm^2 shown in fig. 6 are particularly interesting because they indicate that the crack density for given strain tends to a limiting value with further decrease in temperature. Maximum values for the average crack density for this stress and temperatures -4.8°C , -9.5°C and -14.8°C were estimated from figs. 2 (a), (b), and (c) by extension of the curves to a strain of 2×10^{-2} . This estimated maximum value is presented in fig. 6.

7. The stress dependence of the crack density at a given strain was described with reasonable accuracy by the equation

$$N = A(\sigma - 6)^{1.7} \text{ cracks/cm}^2. \quad \dots \dots (1)$$

where A is a constant, and σ the stress in kg/cm^2 .

8. The number of initial cracks formed for a given stress decreased with decrease in temperature, and the stress that must be exceeded to cause cracks to form increased.

6.1. Statistics of the Cracking Activity

The experiments indicated that when the stress was less than about 10 kg/cm^2 , the cracking activity occurred randomly within the area of observation. A series of experiments was carried out to determine whether this was the case. Three sets of specimens were deformed under a constant compressive stress of 10 kg/cm^2 to strains of 15×10^{-4} , 25×10^{-4} and 50×10^{-4} . Each specimen was subsequently cut to expose the middle plane perpendicular to the long direction of the columns. This surface was polished by slight melting, subdivided into squares 4 cm^2 in area, and the number of cracks intersecting the surface in each square were counted.

The observed distribution in the number of squares containing exactly n cracks was compared to that predicted by assuming the cracking activity was a random process that could be described by the Poisson distribution function. This comparison indicated that the cracking activity was not truly random; the formation of a crack appeared to lower the probability

of a crack being formed subsequently in the same square or in immediately adjacent squares.

The deviation of actual behaviour from random behaviour, although significant, was sufficiently small that it would be reasonable to assume that a specimen could be subdivided into essentially independent regions. From this point of view, one could look at each test as being a set of concurrently run independent experiments on the stress, strain and temperature dependence of the probability for the initiation of a crack within a given region.

Let the probability of a crack forming in a given region be $P(\sigma, \epsilon, T)$; a function of stress, σ ; strain, ϵ ; and temperature, T . Applying the statistics of Weibull (1939, 1951), it can be shown that

$$P = 1 - \exp(-\phi), \dots \dots \dots (2)$$

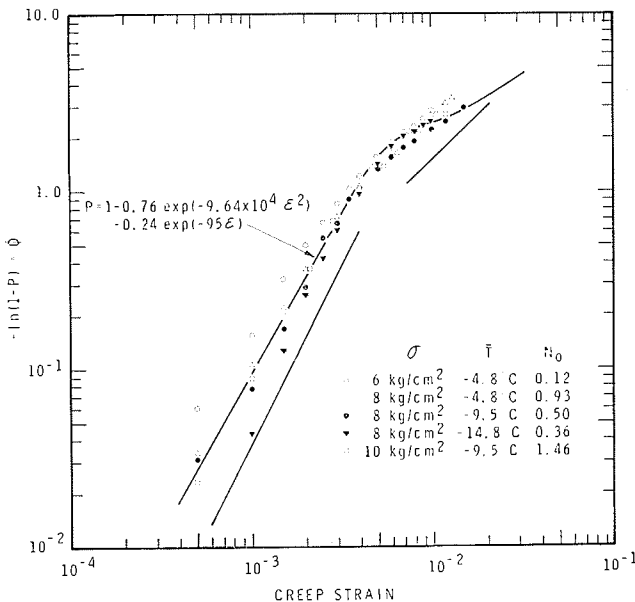
where ϕ is a function of stress, strain and temperature. Assume

$$\phi = \phi_0 \epsilon^m, \dots \dots \dots (3)$$

where m is a constant and ϕ_0 is a function of stress and temperature.

Observations on the strain dependence of the crack density for stress of 6, 8 and 10 kg/cm² were converted into probability distribution functions by dividing by the estimated maximum density. The initial cracks formed on loading the specimens were included in this calculation. In fig. 8, $\log[-\ln(1-P)] = \log \phi$ is plotted against $\log \epsilon$ for each of these distributions. Given also in the figure is the estimated maximum density, N_0 , for each case.

Fig. 8



Log $[-\ln(1-P)]$ versus $\log \epsilon$, $\sigma \leq 10$ kg/cm²; P is the probability distribution for the cracking activity; N_0 is the estimated maximum crack density.

It can be seen that the observations define a curve rather than a straight line, as predicted by eqns. (2) and (3). Lines with slopes, m , equal to 1 and 2 are drawn in fig. 8. The line with slope 2 is approximately parallel to the observations for strains less than 4×10^{-3} ; the line with slope 1, for strains greater than 5×10^{-3} . This suggests that the distribution is of the compound type, made up of two independent distributions (Weibull 1939).

Let the distribution with slope 1 be P_1 , and with slope 2, P_2 . Assume they are present in the proportion α so that

$$P = \alpha P_1 + (1 - \alpha) P_2. \quad \dots \dots \dots (4)$$

This gives

$$P = 1 - \exp(-B\epsilon^2) + \alpha[\exp(-B\epsilon^2) - \exp(-A\epsilon)]. \quad \dots (5)$$

The strains corresponding to $P = 0.9, 0.5$ and 0.2 were determined from the probability distributions in fig. 8 and used to calculate A, B and α in eqn. (5). The resulting equation is presented and plotted in fig. 8. It can be seen that the calculated distribution function does provide a good fit to the observations. It can also be seen that although stress and temperature have a significant effect on N_0 , they have only a secondary effect, if any, on A, B and α for the range covered.

The probability density for the cracking activity is given by

$$\begin{aligned} \frac{\partial P}{\partial \epsilon} &= (1 - \alpha) B \epsilon \exp(-B\epsilon^2) + \alpha A \exp(-A\epsilon), \quad \dots \dots (6) \\ &= \frac{1}{N_0} \frac{\partial N}{\partial \epsilon}. \end{aligned}$$

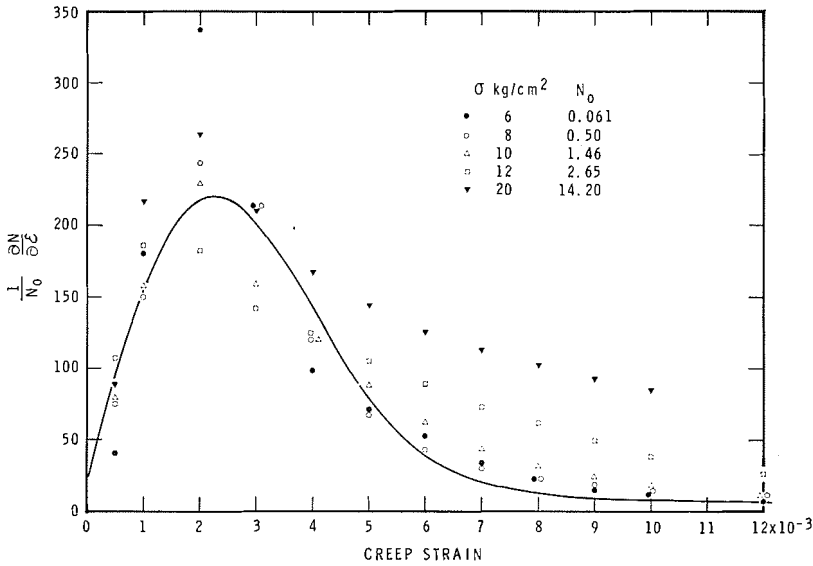
Calculated values of $(1/N_0)(\partial N/\partial \epsilon)$ for temperature -9.5°C and stress of 6, 8 and 10 kg/cm^2 , are plotted in fig. 9. Equation (6) is also plotted in this figure, using the values for α, A and B given in fig. 8.

It was not possible to estimate a value for N_0 for stress $\geq 12 \text{ kg/cm}^2$ because the cracking rate was still relatively high for this condition when the load was removed. The results presented in fig. 8 show, however, that the crack densities at strain ϵ for different stresses hold the same relationship to each other as the maximum densities. It was possible, therefore, to use eqn. (1) to estimate the apparent maximum crack densities for stress $\geq 12 \text{ kg/cm}^2$. The values calculated for $(1/N_0)(\partial N/\partial \epsilon)$ for stress of 12 and 20 kg/cm^2 and temperature -9.5°C are presented in fig. 9. It can be seen that the maximum value for their probability density is in reasonable agreement with that given by eqn. (6). The probability density for these stresses, however, is appreciably greater than that given by the calculated curve for a given strain when it is larger than 50×10^{-4} . The significance of this is considered in the discussion.

§ 7. DISCUSSION

The statistical analysis of the observations on the strain dependence of the crack density has indicated the possibility of two independent families

Fig. 9



The probability density for the cracking activity, $\bar{T} = -9.5^\circ\text{C}$.

of cracks. This is not unreasonable from a physical point of view. The term involving $\phi = B\epsilon^2$ in eqn. (5) implies that the probability for the nucleation of a crack in a region increases directly with strain. Such behaviour could be expected if these cracks were caused by a process such as the pile-up of dislocations. The term with $\phi = A\epsilon$ implies that the probability of nucleation is independent of the strain. This could occur if nuclei of various sizes were present initially, and these grew by an essentially strain-independent process (e.g. by diffusion) or were subject to a gradually increasing local stress.

Equation (6) states that there was a finite probability for crack formation when the load was applied (i.e. creep strain equal to zero), which was associated with the P_1 distribution. It was noted during the study that the cracks formed during this period were mainly at the grain boundaries. The possibility that grain boundary cracking was associated with the P_1 distribution was indicated also by the value obtained for α in eqn. (6) (i.e. 0.24 – see fig. 8). This value was close to the proportion of the total crack population that was observed by Gold (1966) to be grain boundary cracks.

Smith and Barnby (1967) give as a criterion for crack nucleation by the pile-up of dislocations

$$\tau_c > \left[\frac{\pi\gamma E}{4(1-\nu^2)l} \right]^{1/2}, \dots \dots \dots (7)$$

where τ_c is the effective shear stress on a pile-up of length l , E is Young's modulus, ν is Poisson's ratio and γ is the surface energy. Representative values for $E/(1-\nu^2)$ and γ are:

$$\frac{E}{1-\nu^2} = 8.4 \times 10^4 \text{ kg/cm}^2 (8.2 \times 10^9 \text{ N/m}^2) \quad (\text{Gold 1958})$$

$$\gamma = 109 \text{ ergs/cm}^2 (109 \times 10^{-3} \text{ J/m}^2) \quad (\text{Ketcham and Hobbs 1969}).$$

Let the length of the pile-up, l , for the minimum stress to cause crack initiation be made equal to the average grain diameter (0.30 cm). Substituting these values into equation (1), $\tau_c = 4.9 \text{ kg/cm}^2 (4.8 \times 10^5 \text{ N/m}^2)$. This estimate is in good agreement with that which would be calculated from the observed minimum compressive stress associated with cracking activity (i.e. about 3 kg/cm^2), and demonstrates that stress concentrations of this type could cause cracks in ice.

The marked transition that occurred in the creep behaviour over the stress range of 10 to 12 kg/cm^2 suggests that for a given stress there may be a critical crack density which, if exceeded, induces structural instability (allows tertiary creep to begin). An estimate was made of the density at the transition from the secondary or primary stage of creep to the tertiary using the observations of the average strain dependence of the creep rate and crack density. It was found that a density of 1.4 cracks/cm^2 could develop for stress less than or equal to 10 kg/cm^2 without the tertiary stage being initiated in the first 10^{-2} of strain. The rate of change of the creep rate changed from negative to positive for stress of 12 kg/cm^2 when the density was about 1.6 cracks/cm^2 . This occurred at a strain of less than 40×10^{-4} , for which the average spacing between cracks was about 0.80 cm, or about three grain diameters. The tertiary stage of creep was usually associated with non-uniform cracking activity, with the cracks tending to form in zones parallel to the planes of maximum shear.

The initiation of the tertiary stage of creep depends on both the stress and the crack density. Equations (1) and (5) show that the higher the stress, the more significant, initially, would be the contribution of the family of cracks whose probability of formation was independent of strain. If the stress was sufficiently high, presumably the cracks associated with this distribution could alone cause the breakdown in structure required to induce instability.

Observations have been made by Gold and Krausz (1971) of the failure of ice at rates of strain in the region of the transition from ductile to brittle behaviour. The cracking activity was initially random, as it was during creep. For brittle behaviour, failure occurred abruptly by the formation of fault zones, and the ice from the zones was highly shattered. It was observed for brittle behaviour that the cracks were mainly at grain boundaries (unpublished work), indicating that they belonged to the P_1 distribution in eqn. (5). This suggests that the occurrence of the ductile to brittle transition for compressive loads for ice is dependent on the stress dependence and relative contribution of the two families of cracks.

One of the more interesting results of the study was the decrease in crack density with temperature for given stress and strain. Information presented by Ketcham and Hobbs (1969) indicates that the temperature

dependence of the change in surface energy is not sufficient to explain this behaviour. The establishment of the crack-nucleating condition must depend on the crystallographic orientation of the grains in the vicinity of the site, and the relative contribution of the various modes of deformation that are active. Measurement of the apparent activation energy for ice indicates that there is a change over the temperature range of 0 to -40°C in the relative contribution to the strain of these deformation mechanisms (Gold 1970). It is probable that the temperature dependence of the crack density is due to this change.

§ 8. CONCLUSIONS

Cleavage type crack formation occurred in the columnar-grained ice used in the investigation when the uniaxial compressive stress, applied perpendicular to the long axis of the grains, exceeded about 6 kg/cm^2 . The cracking activity depended on stress, strain and temperature, and was maximum in the primary creep stage. For stress less than about 10 kg/cm^2 , the rate of crack formation tended to zero in the secondary creep stage. When the stress exceeded about 12 kg/cm^2 , structural deterioration due to crack formation caused the primary stage of creep to change directly to the tertiary stage.

Prior to the onset of tertiary creep, crack nucleation approximated a depletion-type random process, although the formation of a crack did appear to reduce the probability of a second forming in its vicinity. The strain dependence of the crack density involved two Weibull-type distributions. For one, the probability of nucleation was proportional to strain, and for the other was independent of it. The existence of these two distributions can explain the strain rate dependence of the ductile to brittle transition for ice.

ACKNOWLEDGMENTS

The author gratefully acknowledges helpful discussions with Professor E. R. Pounder and Professor J. J. Jonas.

This paper is a contribution from the Division of Building Research, National Research Council of Canada, and is published with the approval of the Director of the Division.

REFERENCES

- BRACE, W. F., PAULDING, B. W., and SCHOLZ, C., 1966, *J. geophys. Res.*, **71**, 3939.
GOLD, L. W., 1958, *Can. J. Phys.*, **36**, 1265; 1960, *Ibid.*, **38**, 1137; 1965, *Ibid.*, **43**, 141; 1966, *Ibid.*, **44**, 2757; 1970, *The Failure Process in Columnar-Grained Ice*, Ph.D. Thesis, McGill University, Montreal, Quebec, Canada.
GOLD, L. W., and KRAUSZ, A. S., 1971, *Can. Geotech., J.*, **8**, 163.
HILLIG, W. B., 1958, *The Kinetics of Freezing of Ice in the Direction Perpendicular to the Basal Plane*, In *Growth and Perfection of Crystals*, (New York: John Wiley and Sons), p. 350.

- JONES, R., 1962, *Rheol. Acta*, **2**, 34.
KAMB, W. B., 1961, *J. Glac.*, **3**, 1097.
KENNY, P., and CAMPBELL, J. D., 1967, *Prog. Mater. Sci.*, **13**.
KETCHAM, W. M., and HOBBS, P. V., 1969, *Phil. Mag.*, **19**, 1161.
RAMSEIER, R. O., 1968, *J. Crystal Growth*, **3**, **4**, 621.
SMITH, E., and BARNBY, J. T., 1967, *Met. Sci. J.*, **1**, 56.
WEIBULL, W., 1939, *The Phenomenon of Rupture in Solids*, *Proc. R. Swed. Inst. Engng. Res.*, Paper No. 153; 1951, *J. appl. Mech.*, **18**, 293.

This publication is being distributed by the Division of Building Research of the National Research Council of Canada. It should not be reproduced in whole or in part without permission of the original publisher. The Division would be glad to be of assistance in obtaining such permission.

Publications of the Division may be obtained by mailing the appropriate remittance (a Bank, Express, or Post Office Money Order, or a cheque, made payable to the Receiver General of Canada, credit NRC) to the National Research Council of Canada, Ottawa. K1A 0R6. Stamps are not acceptable.

A list of all publications of the Division is available and may be obtained from the Publications Section, Division of Building Research, National Research Council of Canada, Ottawa. K1A 0R6.